Electromagnetic Design for Hard Disk Drive Spindle Motors with Fluid Film Lubricated Bearings

Z. J. Liu, C. Bi*, Q. D. Zhang, M. A. Jabbar and T. S. Low
Magnetics Technology Centre, National University of Singapore, Singapore 0511
Western Digital (S) Pte Ltd, Singapore 1646

Abstract— **This paper discusses the problems associated with the electromagnetic design of hard disk drive (HDD) spindle motor having fluid film bearings. It will highlight the effect of the unbalanced electromagnetic pull in the radial direction of FFB spindle which uses permanent magnet brushless DC motors with slotted stator core. An analytical approach is employed for predicting the magnetic field and motor performance. Results obtained from this approach are compared with finite element analysis.**

I. INTRODUCTION

As the data storage technology advances, there is an increasing demand to develop hard disk drive (HHD) spindles supported by fluid film bearings (FFB) in order to achieve extremely high recording density. The effect of the unbalanced electromagnetic pull is a particular design issue in electromagnetic aspects for such spindles, the common topology of which is permanent magnet brushless (BLDC) motor. Previous studies on such effect were primarily for induction machines in relation to design issues such as vibration and acoustic noises etc. [e.g. 1,2]. An unbalanced electromagnetic pull, or otherwise named the de-centering force by mechanical designers, in a rotating motor can occur when there is an eccentricity between the stator and rotor, which is the normal operation mode for the FFB system, or when the magnetic flux path is not symmetric about the axis of the motor. Since its direction and magnitude are changing with the rotor position, such an unbalanced pull can be a source of vibration and acoustic noise, in addition to the magnetic cogging effect. For FFB spindles, the unbalanced pull affects the rotor dynamics and also the performance of the bearing system as the magnitude of the alternating force can be comparative to the total load of the spindle.

In order to investigate these effects in BLDC machines, an appropriate modeling of the air gap magnetic field is necessary. It is noteworthy that the unbalanced force and cogging torque are strongly related to parasitic flux ripples in the air gap field distribution. Since these ripples normally have very small wavelengths, a high level of node density, especially in the air gap region, is necessary when using finite element analysis to study the de-centering forces and cogging effects. Therefore it is desirable to use an analytical approach which can be used to study the interdependence of the motor parameters and the forth-mentioned effects with much less computer time consumption. It will also be noted that due to a large equivalent air gap length, one-dimensional analytical modeling of the magnetic field in BLDC machines does not generally suffice for providing accurate and reliable information about the machine performance. This paper discusses the electromagnetic design of HHD spindle motors with particular reference to the unbalanced magnetic pull and cogging effects. The spindle has an underslung structure as illustrated in Fig. 1. Analysis results for 8 pole 9 slots and 8 pole 12 slots BLDC motors which are commonly used for HHD systems, are presented. In the study, an analytical model for predicting the magnetic field and electromagnetic forces in brushless dc motors is employed. The analytical model is based on the solution of the two dimensional magnetic field in polar coordinates. It takes into account the effect of the harmonics of the air gap permeance due to slotting of the stator core. Magnetic forces and torque can be obtained from the solution by using directly the Maxwell method without further assumptions [e.g. 3,4]. The effects of the pole-slot number combination and the rotor positions are reflected in the analytical model. The results shows that the magnitude of the alternating magnetic pull can be too large to be neglected as compared to the total load of the disk drive spindles and its effect should be properly taken into account in the electromagnetic design of the spindle motors. The computed results obtained from this model are compared with the predictions obtained from finite element analysis.

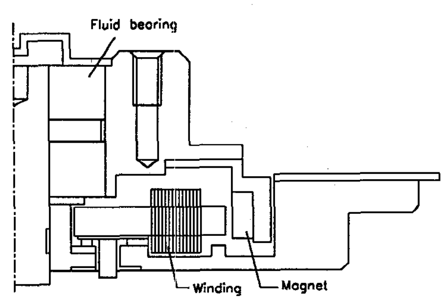

Fig. 1 Structure of underslung HDD spindle

II SOLUTION OF MAGNETIC FIELD PROBLEM

The geometry of the cylindrical machine with rotating magnet poles is illustrated in Fig. 2, in which the definitions of the polar coordinate system and the symbols used in the analysis are also indicated. In order to simplify the analysis, the permeability of the rotor back iron is assumed to be infinite. Thus the solution domain can be subdivided into two regions: Region I, the machine air gap, and Region II, the magnet poles. The magnetic vector potential can be used to describe the 2-d electromagnetic in the polar coordinates:

for air gap $$\frac{\partial^2 A_1}{\partial r^2} + \frac{1}{r}\frac{\partial A_1}{\partial r} + \frac{1}{r^2}\frac{\partial^2 A_1}{\partial \theta^2} = 0 \quad (1)$$

Manuscript received on 4 March 1996

0018-9464/96$05.00 © 1996 IEEE

$$\text{for magnet} \quad \frac{\partial^2 A_2}{\partial r^2} + \frac{1}{r}\frac{\partial A_2}{\partial r} + \frac{1}{r^2}\frac{\partial^2 A_2}{\partial \theta^2} = \frac{\mu_0}{r}\frac{\partial M_r}{\partial \theta} \qquad (2)$$

where μ_0 is the permeability of air and M_r is the magnetization of magnet poles and can be represented by the Fourier expansion.

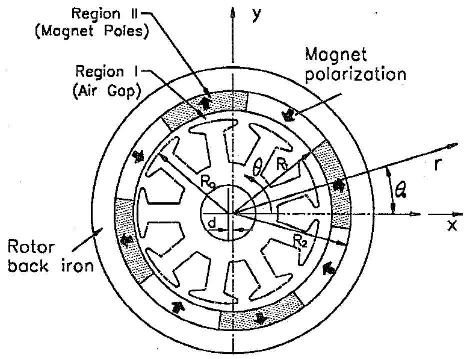

Fig. 2 Cross-sectional view of PM BLDC spindle motor

The boundary condition at R_2 is $H_\theta = 0$ due to the assumed infinite permeability for the rotor back iron, and the boundary condition at R_0 is represented by:

$$B_r = f(\theta) = \sum_{n}^{\infty} \sum_{m}^{\infty} B_{nm} \cos(np \pm mq)\theta \qquad (3)$$

The above boundary condition defines the radial component of the flux density at the outer surface of rotor laminations which is slotted. The function $f(\theta)$ is the multiplication of two periodic functions, one with the period $2\times\tau$, i.e. the full pole pitach, and the other with the period τ_t, which is the stator tooth pitch, since the magnetic field is under the influence of the magnet poles, and the slotting of the stator core. In Equ. (3), the amplitude B_{nm} can be obtained by using the concept of air gap permeance and expressed as

$$B_{nm} = -\frac{a_n}{(1-n^2)G'_n} \left[(n+1)\frac{R_2^{\,n}}{R_1^{\,n}} R_1 - (n-1)\frac{R_1^{\,2n}}{R_2^{\,2n}} R_1 - 2R_2 \right] \frac{R_0^{\,n}}{R_1^{\,n}} \lambda_m$$

$$G'_n = \left[(\mu_2+1)\left(1 - \frac{R_0^{\,2n}}{R_2^{\,2n}}\right) + (\mu_2-1)\left(\frac{R_1^{\,2n}}{R_2^{\,2n}} - \frac{R_0^{\,2n}}{R_1^{\,2n}}\right) \right]$$

The relative permeance can be calculated using conformal transformation approach for slotted stator core [5].

Taking into account the rotor position, as described by ϑ_0 the angle between the reference frame of the rotor and the stator as shown in Fig. 2, the general solution of the boundary value problem may be given in the following expressions:

$$A_1(r,\theta) = \sum_{n}^{\infty}\sum_{m}^{\infty} [C_{1N} r^{N} + D_{1N} r^{-N}] \, [\sin n\vartheta_0 \cos N\theta + \cos n\vartheta_0 \sin N\theta] \qquad (3)$$

$$A_2(r,\theta) = \sum_{n}^{\infty}\sum_{m}^{\infty} [C_{2N} r^{N} + D_{2N} r^{-N}] \, [\sin n\vartheta_0 \cos N\theta + \cos n\vartheta_0 \sin N\theta] \qquad (4)$$

where N=np± mq, n = 1, 3, 5, ..., and m = 1, 2, 3, 4, 5,..., q is the number of slots, and p is the number of pole pairs. The periodicity of the magnetic field under investigation has already been considered in the expressions (3) and (4). The arbitrary constants can be found from the boundary conditions.

III CALCULATION OF MAGNETIC FORCES

Clearly, the general solution described in the last section allows the radial as well as the tangential components of the magnetic flux density to be readily obtained, as given by the following relations: $B_r = 1/r(\partial A/\partial\vartheta)$ for the radial component and $B_r = -(\partial A/\partial r)$ for the tangential component. Hence the components of the radial magnetic force in the x and y directions (See Fig. 2) can be calculated by:

$$F_x = \frac{L}{g\mu_0}\int_{r_0}^{r_1} dr \int_{-\pi}^{+\pi} [0.5(B_r^{\,2} - B_\theta^{\,2})\cos\theta - B_r B_\theta \sin\theta] d\theta$$

$$F_y = \frac{L}{g\mu_0}\int_{r_0}^{r_1} dr \int_{-\pi}^{+\pi} [0.5(B_r^{\,2} - B_\theta^{\,2})\sin\theta + B_r B_\theta \cos\theta] d\theta$$

where L is the effective length of the stator core, and g is the length of the air gap. The torque can also be obtained similarly by using the Maxwell method. It can be found that, after the integration according to the above equations, only the harmonics components whose orders satisfy the relation np±mq±1 may have effect to the resultant unbalanced force. Therefore, if the number of slots is even, the radial force counter-balances and becomes zero unless there is an offset between the rotor and stator centres.

When there is an offset, d, between the centres of the stator and rotor, as shown in Fig. 2, the air gap field will be affected. The influence of this offset can be effectively accounted for by modifying the relative permeance for the air gap, such that [6]:

$$\lambda(\theta) = \nu(1+\varepsilon)\sum_{m}^{\infty} \lambda_m \cos(mq\theta)$$

where $\nu = 1/(1-0.5\varepsilon^2)$, $\varepsilon = d/g$ is the eccentricity.

Computational results are presented below for 8 pole 12 slot and 8 pole 9 slot BLDC motors used in the underslung HHD spindles. The main parameters are as follows: R_0 = 15.2 mm, R_1 = 15.6 mm, R_2 = 17.1 mm, and L= 4 mm. The magnet poles are made of plastic bonded NdFeB magnet having a remanance of B_R = 0.72 (T). The total load of the spindle is about 2 N during operation.

Fig. 3 shows the distribution of the air gap flux density distribution against θ at ϑ_0 = 40.5° mechanical degree and $r = R_0$ + g/2, i.e. the centre of the air gap, for the 8 pole 12 slot motor. The solid curve represents the results computed by using the analytical model, which agree well with the results, showing by squares, obtained from finite element analysis assuming infinite permeability for the rotor back iron. The effect of the stator slotting can be clearly observed from this figure.

The predictions of the unbalanced pull as a function of the rotor position ϑ_0 is illustrated in Fig. 4. The solid curve is the x-component and the dashed curve is the y-component. The rotor position ϑ_0 varies from 0 to π/2 mechanically. This unbalanced pull is due to the stator core slotting which makes the magnetic flux path non-symmetric about the centre of the motor. The computed results indicate that the peak to peak value of this alternating force is about 0.8 N, comparing to the total load of the spindle of 2 N. Furthermore when the spindle shaft is vertically oriented, the alternating unbalanced force becomes the main radial force component that affects the performance of the journal fluid film bearing. However, it is known to motor designers that torque developed in an 8 pole 9 slot BLDC motor contains smaller ripples. This advantage makes it a candidate among the design options for HDD spindles. Fig. 5 shows a comparison between the cogging torque profiles for 8 pole 12 slot and 8 pole 9 slot motors. Measures, for example pole skewing, must be taken in order to reduce the magnitude of the cogging torque ripple when 8 pole 12 slot motor is to be used in practice. It will be noted that since the wavelength of the torque ripple for the 8 pole 9 slot motor is only 5° mechanical degree, a very high mesh density is needed to include the effects of high order magnetic flux pulsation and to capture the peak values of the torque ripple when using conventional finite element method.

The effect of the rotor eccentricity on the unbalanced magnetic pull is shown in Fig. 6 by plotting the magnitude of the de-centering force against the offset, d, varies from 1 to 16 microns which is about the normal working range of the fluid film bearings designed for HHD spindles. It can be seen that this force is also significant enough as compared to the total load of the spindle.

IV CONCLUSIONS

The electromagnetic design of HHD spindle motors is discussed with particular reference to the effects of radial and tangential magnetic forces due to the stator core slotting and the rotor eccentricity. The study is based on an analytical model suitable for predicting magnetic fields in PM BLDC motors. The technique provides a fast design and analysis tool for evaluating the magnetic forces which is otherwise a very time-consuming task if using a conventional finite element method. The results indicate that the magnitudes of the unbalanced pull due to slotting of the stator core or the eccentricity can be large enough comparing to the total load of the HDD spindles. Therefore, the effect should be properly taken into account in the design stage of HDD spindle motors supported by fluid film bearings.

REFERENCES:

[1] K. J. Binns, and P. A. Kahan, "Effects of load on the flux pulsations and radial-force pulsations of induction motor teeth", *IEE Proc*, vol. 127, Pt. B, No. 4, pp 223-230, 1980

[2] A. Arkkio, "Unbalanced magnetic pull in a four-pole induction motor with an odd number of rotor slots", *Proc. of the 2nd Chinese International Conference on Electrical Machines*, Hangzhou, China, Aug. 31- Sept. 2, 1995, pp. 343-348.

[3] N. Boules, "Prediction of no-load flux density distribution in permanent magnet machines", *IEEE Trans. Ind. Appl.* vol. 21, No., 3, pp. 633-643, 1985.

[4] Z. Q. Zhu, and D. Howe, "Analytical prediction of cogging torque in radial-field permanent magnet brushless motors", *IEEE Trans., Magn.*, vol. 28, No. 1, pp. 1080-1083, 1992.

[5] K. J. Binns, P. J. Lawrenson, and C. W. Trowbridge, "The analytical and numerical solution of electric and magnetic fields', John Wiley and Sons, 1992.

[6] B. Heller, and V. Hamata, "Harmonic field effects in induction machines", Elsevier, 1977.

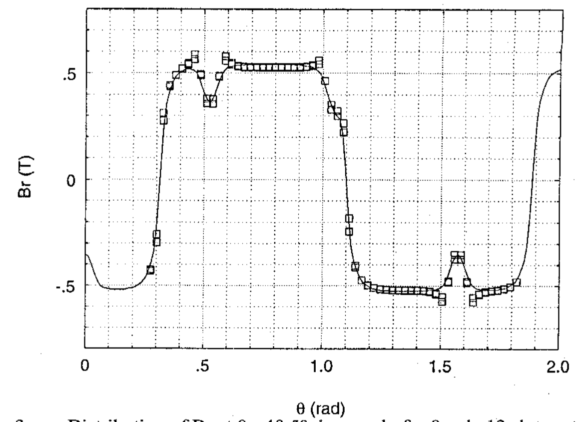

Fig. 3 Distribution of Br at θ= 40.5° deg mech. for 8 pole 12 slot motor

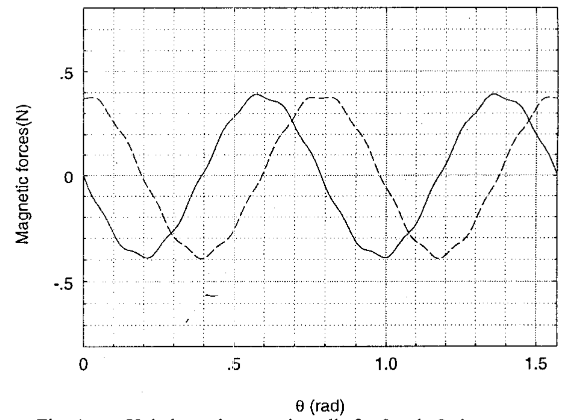

Fig. 4 Unbalanced magnetic pulls for 8 pole 9 slot motor

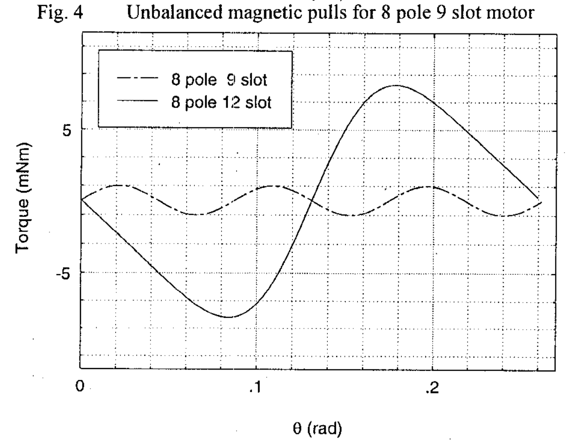

Fig. 5 Cogging torque profiles for PM BLDC motors

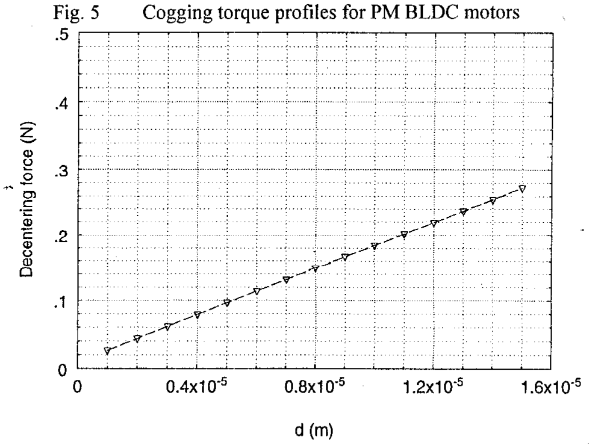

Fig. 6 De-centering force vs. rotor eccentricity d